Detachment-activated FAK-STAT3-NNMT inhibits anoikis by enhancing fatty acid oxidation in breast cancer

Qingchao Tong
Zhejiang University School of Medicine
Yilei Ma
Sir Run Run Shaw Hospital
Yuzhen Gao
Sir Run Run Shaw Hospital
Lin Zhou
Sir Run Run Shaw Hospital
Qiang Fang
Sir Run Run Shaw Hospital
Sining Fang
Sir Run Run Shaw Hospital
Ru Zhao
Sir Run Run Shaw Hospital
Jin Zeng
Sir Run Run Shaw Hospital
Guoli Li
Sir Run Run Shaw Hospital
Xinyou Xie
Sir Run Run Shaw Hospital
Yanzhong Wang
Sir Run Run Shaw Hospital
Jun Zhang (jameszhang2000@zju.edu.cn)
Sir Run Run Shaw Hospital

Research Article

Keywords: anoikis, breast cancer, NNMT, FAO

Posted Date: February 12th, 2024

DOI: https://doi.org/10.21203/rs.3.rs-3933796/v1

Additional Declarations: No competing interests reported.

Detachment-activated FAK-STAT3-NNMT inhibits anoikis by enhancing fatty acid oxidation in breast cancer

Qingchao Tong[1,2,*], Yilei Ma[1,2,*], Yuzhen Gao[1,2], Lin Zhou[1], Qiang Fang[1], Sining Fang[1,2], Ru Zhao[1,2], Jin Zeng[1,2], Guoli Li[1,2], Xinyou Xie[1,2], Yanzhong Wang[1,2,#], Jun Zhang[1,2,#]

1 Department of Clinical Laboratory, Sir Run Run Shaw Hospital, Zhejiang University School of Medicine, Hangzhou, Zhejiang, PR China

2 Key Laboratory of Precision Medicine in Diagnosis and Monitoring Research of Zhejiang Province, Hangzhou, Zhejiang, PR China

* These authors contributed equally to this work and should be considered as co-first authors.

# These authors contributed equally to this work and should be considered as co-corresponding authors.

<u>*Corresponding Author:</u>

Jun Zhang (Corresponding author)

Department of Clinical Laboratory, Sir Run Run Shaw Hospital, Zhejiang University School of Medicine, 3 East Qingchun Road, Hangzhou 310016, Zhejiang, People's Republic of China.

E-mail: jameszhang2000@zju.edu.cn

Tel.: +86-0571-86002260

Fax: +86-0571-86044817

Yanzhong Wang (Co-corresponding author)

Department of Clinical Laboratory, Sir Run Run Shaw Hospital, Zhejiang University School of Medicine, 3 East Qingchun Road, Hangzhou 310016, Zhejiang, People's Republic of China.

E-mail: jonnhy2021@zju.edu.cn

Tel.: +86-0571-86002260

Fax: +86-0571-86044817

Abstract

Purpose: Breast cancer metastasis claims the majority of breast cancer-related deaths. Anoikis resistance is a key prerequisite for tumor metastasis. Possible mechanism of evading anoikis in breast cancer remains unclear. Our previous research demonstrated that Nicotinamide N-methyltransferase (NNMT) has essential functions in cancer development and metastasis. However, the spercific functional mechanisms of NNMT in breast cancer anoikisp remain to be explored

Method: Immunofluorescence staining, confocal microscopy analysis, immunoblotting and qPCR were used to analyze NNMT expression. Flow cytometry and soft agar assay were used to analyze the proportion of breast cancer cells undergoing anoikis. ChIP assay and detached cell model were used to confirm the presence of FAK-STAT3-NNMT in detached breast cancer cells. BODIPY staining was used to visualize lipid deposit in the cytoplasm, and Seahorse analysis was used to directly measure FAO rate of attached and detached breast cancer cells.

Results: Detachment of breast cancer cells activates the FAK-STAT3 axis to increase the transcription of NNMT, which then protects breast cancer cells from anoikis by enhancing fatty acid oxidation (FAO). Mechanistically, NNMT promotes the expression of CPT1A, a FAO rate-limiting gene, by suppressing PP2A methylation. Furthermore, NNMT-induced FAO accelerates the clearance of reactive oxygen species (ROS), which triggers anoikis and hinders cancer metastasis, by maintaining $NADP^+$/NADPH balance. *In vivo* experiments show that NNMT-knockdown breast cancer cells colonize the lung much less than that of NNMT high expression cells. Additionally, inhibitors of NNMT or FAO suppressed breast cancer cell metastasis, suggesting that NNMT-mediated FAO enhances the metastatic potential of breast cancer.

Conclusion: Our study identifies that NNMT, an enzyme upregulated during detachment via the FAK-STAT3 axis, activates the FAO pathway to resist anoikis of breast cancer cells.

Keywords: anoikis, breast cancer, NNMT, FAO

1. Background

Female breast cancer has now become the most frequently diagnosed cancer, surpassing lung cancer, with an estimated 2.3 million new cases (11.7%)[1]. The spread of advanced breast cancer to other organs such as lung, liver, brain, or bone is a common occurrence, ultimately compromising organ function and causing patient morbidity mortality[2]. It's reported that 20–30% of breast cancer patients develop metastases after diagnosis and primary tumor treatment, and that approximately 90% of cancer-related deaths can be attributed to metastasis[3]. Hence, identifying and characterizing critical signaling pathways associated with metastasis in breast cancer is a high priority.

Extracellular matrix (ECM) detachment will activate several signaling pathways resulting in the activation of caspases and cell death, termed as anoikis[4]. As a subset of apoptosis, anoikis is a major obstacle to cancer metastasis. Only metastatic cancer cells able to evade anoikis can disseminate to distinct organs[5] Upon detachment from the ECM, cells undergo energetic stresses owing to impaired glucose uptake and ATP production[6]. Cancer cells must rectify metabolic deficiencies to meet energy demands and prevent anoikis during ECM detachment. Recent research has revealed that FAO provides an important survival advantage for cancer development by supplying NADH, NADPH, and ATP[7]. Colorectal cancer uses FAO-derived energy to resist anoikis while spreading to

the liver, suggesting that FAO may play a critical role during ECM detachment[8].In breast cancer, FAO has been found to contribute to cancer development such as proliferation, cancer stemness, and chemoresistance[9], particularly under metabolic stress conditions or nutrient restriction[10]. However, the precise function of FAO in breast cancer anoikis resistance and metastasis is yet to be fully understood.

Nicotinamide N-methyltransferase (NNMT) is an intracellular enzyme that catalyzes the transfer of methyl group from S-adenosyl-L-methionine (SAM) to nicotinamide (NA), generating S-adenosylhomocysteine (SAH) and 1-methylnicotinamide (1-MNA). NNMT has been reported to be upregulated in various types of cancer including prostate cancer[11], colon cancer[12], breast cancer[13], and a high level of NNMT positively correlated with cancer cell metastasis[14], proliferation[15], and chemotherapy resistance[16]. In addition to the well-known role of NNMT in regulating histone, non-histone proteins, and DNA methylation capacity[17], researchers have recently uncovered its involvement in cellular energy metabolism. For instance, Kraus's study linked NNMT to obesity and fatty acid metabolism of adipose tissue[18], Eckert's work demonstrated that NNMT served as a major metabolic regulator of ovarian cancer-associated fibroblasts[19], and Cui's research indicated that NNMT regulated metabolic reprogramming and promoted the Warburg effect in esophageal squamous cell carcinoma[20]. As such, the impact of NNMT on FAO in breast cancer is still uncertain.

Thus, while the role of NNMT in promoting metastasis has been recognized across several types of cancer, as noted**[13,21,22]**, the underlying mechanisms by which NNMT potentiates breast cancer cell metastasis remain to be elucidated. Therefore, in this study, we observed the upregulation of NNMT in detached breast cancer cells via the FAK-STAT3 axis. Further experiments revealed that NNMT-mediated FAO plays a crucial role in breast cancer resistance to anoikis. However, inhibition of the NNMT-FAO axis using etomoxir, an irreversible small molecule inhibitor of carnitine palmitoyltransferase 1A (CPT1A), exhibited a significant inhibitory effect on cancer metastasis, as compared with control group, indicating the possibility of targeting the NNMT-FAO axis as a potential therapeutic strategy for metastatic breast cancer.

2. Methods

97 2.1 Cell lines and cell culture

98 Human breast cancer cell lines BT-549, MDA-MB-231, HCC1937, and MCF-7 were purchased from
99 the American Type Culture Collection (ATCC, USA). MDA-MB-231 and MCF-7 were cultured in
100 DMEM medium (Gibco, USA). HCC1937 cells were grown in RPMI1640 medium (Gibco), and BT-
101 549 cells were cultured in RPMI1640 medium containing 0.023 U/mL insulin. All mediums were
102 supplemented with 10% FBS (Gibco), 100 U/mL of penicillin, and streptomycin (Sigma-Aldrich).
103 Cells were maintained in a humidified incubator supplemented with 5% CO_2 at 37 °C.

104 2.2 Reagents and antibodies

105 Lipid mixtures were obtained from Sigma-Aldrich(#L2088). BODIPY™ FL C16 was purchased from
106 Thermo Fisher Scientific(#D3821). DCF-DA was purchased from Thermo Fisher Scientific(#D2935).
107 DHE was purchased from Applygen (#C1300-2). PF-562271(#S2890), MK2206(#S1078), 10074-
108 G5(#S8426), and C188-9(S8605) were purchased from Selleckchem. PPZ(HY-A0077A) and OA
109 (#HY-N6785) were purchased from MCE. The antibodies used for Western blot analysis were as
110 follows: anti-β-actin (#4970), anti-P-STAT3(#9145), anti-STAT3(#9139), anti-FAK(#3285), anti-P-
111 FAK(#8556), anti-CPT1A (#12252), anti-CD36 (#14347), anti-P-AKT (#4060), anti-AKT(#9272),
112 anti-PARP(#9532), anti-C-myc(#18583), anti-PP2A(#2038) (Cell Signaling Technology), anti-
113 methylation-PP2A(sc-81603) (Santa Cruz Biotechnology), and anti-NNMT(1E7) obtained as
114 previously described[23].

115 2.3 Tissue and blood RNA-seq data of Breast Cancer Patient Dataset

116 To explore whether NNMT is expressed in the nesting cells of breast cancer, we collected sequencing
117 data from three sources of breast cancer, namely, in situ tissue, peripheral blood Circulating tumor cells
118 (CTCs), and metastatic lesions such as metastatic breast cancer. RNA-seq sequencing data of in situ
119 breast cancer and metastatic breast cancer are from GSE209998; CTC and metastatic breast cancer
120 sequencing data are from GSE113890. After conversion of raw counts to FPKM data of each queue,
121 we used the “sva” package in R to adjust gene expression in all samples. We then used PCA to
122 visualize the status of batching, finally getting the gene expression of three positions. Supplementary
123 Table 1 shows the corrected clinical data.

124 2.4 CTCs differential gene and function enrichment

Through the combined cohort, we used the limma package for differential gene analysis on the sequencing results of CTC versus in situ tissue source samples, using the following standard logFC>0 and P<0.05. The significant difference gene (DEG) of its CTC group was analyzed by enrichGO for pathway function enrichment, and the criterion of pathway difference was q-value<0.05 and p-ajust<0.05

2.5 FAO score

Three breast cancer cohorts, GSE4922, GSE9893, and GSE24450, were obtained to detect the correlation between NNMT and FAO pathways. The functional gene of the FAO pathway was derived from the MSigDB database. Its full name was FATTY_ ACID_ OXIDATION which contained 18 genes, including ACADM, ACADS, ACADVL, ADIPOR1, ADIPOR2, ALOX12, BDH2, CPT1A, CPT1B, ECH1, ECHS1, HACL1, HADHB, HAO1, HAO2, PPARA, PPARD, and PPARGC1A. The single sample enrichment analysis (ssGSEA method) was used to analyze all chips or sequencing data. Supplementary Table 3 lists the enrichment results of the P-adjust<0.001 pathway.

2.6 Quantitative real-time PCR

Total RNA was isolated with TRIzol reagent (Invitrogen). Then, RNA was reverse transcribed into cDNA using the HiFiScript cDNA Synthesis Kit (CWBio). Target mRNA levels were measured with the NovoStart SYBR qPCR SuperMix Plus Kit (Novoprotein). Relative expression levels were calculated using the $2^{-\Delta\Delta Ct}$ method. Data were normalized to β-actin levels. The primer sequences used were listed in Supplementary Table 4.

2.7 Western blot analysis

Total protein was extracted with RIPA buffer (Beyotime Biotechnology) and the concentration of protein was measured with the BCA kit (Multi Sciences). Then Western blot analysis was performed as described[24]. The primary antibodies for β-actin(1:1000), NNMT(1:500), STAT3(1:1000), P-STAT3(1:1000), P-AKT(1:1000), c-myc(1:1000), FAK(1:1000), P-FAK(1:1000), CPT1A (1:1000), CD36 (1:1000), PARP (1:1000), , PP2A(1:1000), and Me-PP2A(1:500) were used.

2.8 BODIPY staining assay

151 To measure lipid deposit, breast cancer cells were first stained with PBS containing 0.1 μg/ml
152 BODIPY™ FL C16 for 20 min at 37°C. After incubation, cells were washed by PBS 3 times, followed
153 by paraformaldehyde fixation. Then cells were stained with DAPI. Images were taken with a confocal
154 microscope. For lipid uptake assay, breast cancer cells were first cultured in serum-free medium for 18
155 hours. Then cells were treated with 2% lipid mixture for 4 hours. After incubation, cells were washed
156 by PBS for 3 times and BODIPY staining was performed as described above.

157 2.9 Soft agar assay

158 Before the experiment, solidified culture medium containing 0.7% agarose was poured into six-well
159 plate. 4-6×10^4 breast cancer cells and reagent (lipid mixture or etomoxir) were mixed with culture
160 medium containing 0.35% agarose before being added to the solidified culture medium. After
161 solidification, 1mL culture medium with lipid mixture or etomoxir was added to the top layer. The
162 culture medium containing the reagent was changed every 2-3 days. After 2-3 weeks, images were
163 taken with a Carl Zeiss Microscope.

164 2.10 Anoikis assay

165 The proportion of detached breast cancer cells undergoing anoikis was determined using a 7-AAD/PI
166 kit (Multi Science, 70-AP105-100). Cells were cultured on a 1% agar-treated plate as described[25] for
167 48 hours. First, cells were collected and washed twice with PBS. Then cells were stained away from
168 light for 30 min at room temperature, before analysis by flow cytometry (FACSCalibur flow cytometer;
169 BD Biosciences).

170 2.11 ChIP assay

171 Samples for ChIP experiments were prepared using SimpleChIP Plus Enzymatic chromatin IP kit
172 (#9005, Cell Signaling Technology) according to the manufacturer's protocol. ChIP experiments were
173 performed with anti-P-STAT3 antibody (#9040, Cell Signaling Technology) and anti-IgG. PCR and
174 qPCR primers for NNMT promoter are described respectively in Supplementary Table 4.

175 2.12 H&E staining and Immunohistochemistry

176 First, tissue samples were fixed in formalin and embedded with paraffin. The paraffin-embedded tissue
177 samples were cut into 4μm-thick sections and then baked at 65 °C for 2h. After deparaffinization and

178 hydration, sections were treated with 0.01 M citrate buffer pH 6.0, and microwave heat induction. Then,
179 the sections were treated with 1% H_2O_2 for 5 mins. After washing with PBS, BSA was used to block
180 non-specific binding for 10 mins. The sections were incubated with anti-CPT1A (Abcam, ab128568,
181 dilution 1:200) and anti-NNMT (1E7, 1:200) in a moist chamber and then with a biotinylated
182 secondary antibody for 30 minutes. Subsequently, the sections were visualized by freshly prepared
183 diaminobenzidine (DAB) and counterstained with hematoxylin. Finally, the images were captured by
184 the digital slide scanning system.

185 2.13 Cellular ROS detection

186 Briefly, breast cancer cells were collected and trypsinized as a single-cell suspension. Then the cells
187 were stained with 1μM DCFH-DA or DHE to avoid the interference from the green fluorescence of
188 lentivirus. Subsequently, cells were incubated at 37 °C for 30 min and washed twice with culture
189 medium before detection via flow cytometry.

190 2.14 Seahorse FAO analysis

191 FAO rate was measured by the Seahorse XF96e Extracellular Flux Analyzer (Agilent Technologies).
192 Breast cancer cells were incubated on agar plates or normal plates for 48 hours before being harvested.
193 Briefly, breast cancer cells were first cultured in XF cell culture microplates with the typical medium.
194 Before starting, cells were cultured in substrate-limited medium for 16 hours. At 45 mins before the
195 assay, cells were washed twice and then cultured with FAO assay medium. Just before starting the
196 assay, 30μl XF palmitate-BSA, as FAO substrate, or BSA was added. Finally, the oxygen consumption
197 rate (OCR) was detected with Mito stress test protocols on Seahorse XF96e Extracellular Flux
198 Analyzer. The FAO rate was normalized to protein levels in each well.

199 2.15 Measurement of cellular NADPH/$NADP^+$ ratios

200 Total cellular NADPH/NADP+ ratios were determined by Amplite™ Colorimetric NADP/NADPH
201 Ratio Assay Kit (AAT Bio, 15274). The experiments were performed according to the manufacturer's
202 protocol.

203 2.16 CTCs isolation and quantification

204 As CTCs model, female SCID mice (6–8 weeks old) were injected into the fourth mammary fat pad
205 with a suspension of 5×10^6 MDA-MB-231 shNC or shNNMT cells in 100μl PBS mixed with matrix
206 gel. 8 weeks later, blood samples were harvested and then shipped to Wastonbiotech where RBC lysis
207 was performed with ammonium chloride solution. After centrifugation, all nucleated cells were
208 deposited on up to 12 glass slides at a concentration of 3×10^6 cells/slide, followed by
209 immunofluorescence staining with Pan-cytokeratin (CK), NNMT, and DAPI. An automated
210 fluorescence microscope (Nikon) was used to verify the localization and staining of CTCs. CTCs were
211 defined as Pan-CK^+ and $DAPI^+$, and CK^- and $DAPI^+$ cells indicate white blood cells

212 2.17 Metastasis animal model

213 Female SCID mice or C57/BL6 micec (6–8 weeks old) were obtained from the Model Animal
214 Research Center of Nanjing University and housed under pathogen-free conditions on a 12/12 h
215 light/dark cycle with free access to food and water. For the MDA-MB-231 metastasis model 1.5×10^6
216 MDA-MB-231 cells suspended in 100μL PBS were injected into SCID mice through the tail vein.
217 Vehicle or 40mg/kg etomoxir was injected intraperitoneally every 2 days and mice were weighed every
218 week before sacrificed. At the endpoint, respective metastatic organs were harvested and metastasis
219 was confirmed by H&E staining. For the E0771 metastasis model, 5×10^5 E0771 vector or NNMT-
220 overexpression cells suspended in 100μL PBS were injected into C57/BL6 mice through the tail vein.
221 Cells were treated with etomoxir 2 days before injection, and vehicle or 40mg/kg etomoxir were
222 injected intraperitoneally every 2 days. The lungs were harvested for H&E staining and IHC after 2
223 weeks. For the MCF-7 metatstasis assay in vivo, MCF-7 vector and NNMT-OE cells were labeled with
224 CellTracker Green (C2925, ThermoFisher) and injected into SCID mice via the tail vein. For the
225 etomoxir treatment group, cells were treated with etomoxir 2 days before injection. Lung tissues were
226 collected at 4 hours and 24 hours after injection and then processed into frozen sections, which were
227 stained with DAPI for fluorescence microscopy.

228 2.18 Statistical analysis

229 Statistical analysis was performed using SPSS 22.0. Statistical significance between groups was
230 calculated by a two-tailed Student's test. Significance values are *$P < 0.05$, **$P < 0.01$, ***$P < 0.001$,
231 and ****$P < 0.0001$. The difference analysis in NNMT RNA expression among multiple groups was

232 tested by the Kruskal-Wallis test in R and adjusted by the Bonferroni method between two groups. In
233 the sequencing queue, Spearman's rank correlation coefficient was used to correlate NNMT and FAO
234 with a statistical difference of $P<0.05$.

235

236 **3. Results**

237 **3.1 ECM detachment induces NNMT transcription through activation of the FAK-STAT3 axis in**
238 **breast cancer cells**

239 To investigate whether NNMT is involved in anoikis resulting from ECM detachment, we analyzed
240 sequencing data from three sources of breast cancer in two queues: primary tumor, peripheral CTCs,
241 and metastatic tumor. Through sva data, we can see that sequencing data of the two queues have been
242 well corrected (Fig. 1A). After extracting NNMT data, we found that the expression of NNMT in CTCs
243 was significantly higher than that of in situ breast cancer samples, but also substantially lower than that
244 of metastatic lesions (Fig. 1A). Consistently, NNMT showed noticeably higher stained in the tumor-
245 invading edge than that of the corresponding tumor region (Fig. 1B), suggesting that NNMT may
246 facilitate cancer cell survival upon detachment from the primary ECM. To further verify these results,
247 we established a CTC model by injecting MDA-MB-231 breast cancer cells into the mammary fat pads
248 of SCID mice, and we found that NNMT expression was, indeed, increased in CTCs compared with
249 MDA-MB-231 by immunofluorescence assay (Fig. 1C). Next, we cultured breast cancer cell lines in
250 suspension for 48h and performed WB and qPCR. Results showed that NNMT expression was
251 significantly higher in detached breast cancer cells compared to that in attached cells (Fig. 1D-E).
252 These results confirmed that NNMT was upregulated in breast cancer cells during detachment.
253 Moreover, we noticed that FAK and STAT3 were both activated in detached breast cancer cells (Fig.
254 1D), and that correspondently, a positive correlation existed between the expression of STAT3 and
255 FAK in breast cancer and pan-cancer (Supplementary Fig. 1A-C). Since STAT3 was one upstream
256 regulator of NNMT[26] and could be activated by the integrin/FAK axis upon ECM detachment[27],
257 we hypothesized that there exists a FAK-STAT3-NNMT axis that upregulates NNMT during ECM
258 detachment. To verify our hypothesis, we treated detached breast cancer cells with FAK inhibitor
259 PF562271 and P-STAT3 inhibitor C188-9. Both qPCR and WB results showed that upregulation of

260 NNMT in detached cells was induced by the FAK-STAT3 axis (Fig. 1F-G). To further confirm our
261 hypothesis, we performed a ChIP assay to directly probe the binding of P-STAT3 to NNMT promoter
262 in detached breast cancer cells (Fig. 1H-I). According to our findings, the upregulation of NNMT in
263 detached cancer cells may be caused by the activation of FAK-STAT3 axis, but its role in detached
264 breast cancer cells remains unclear.

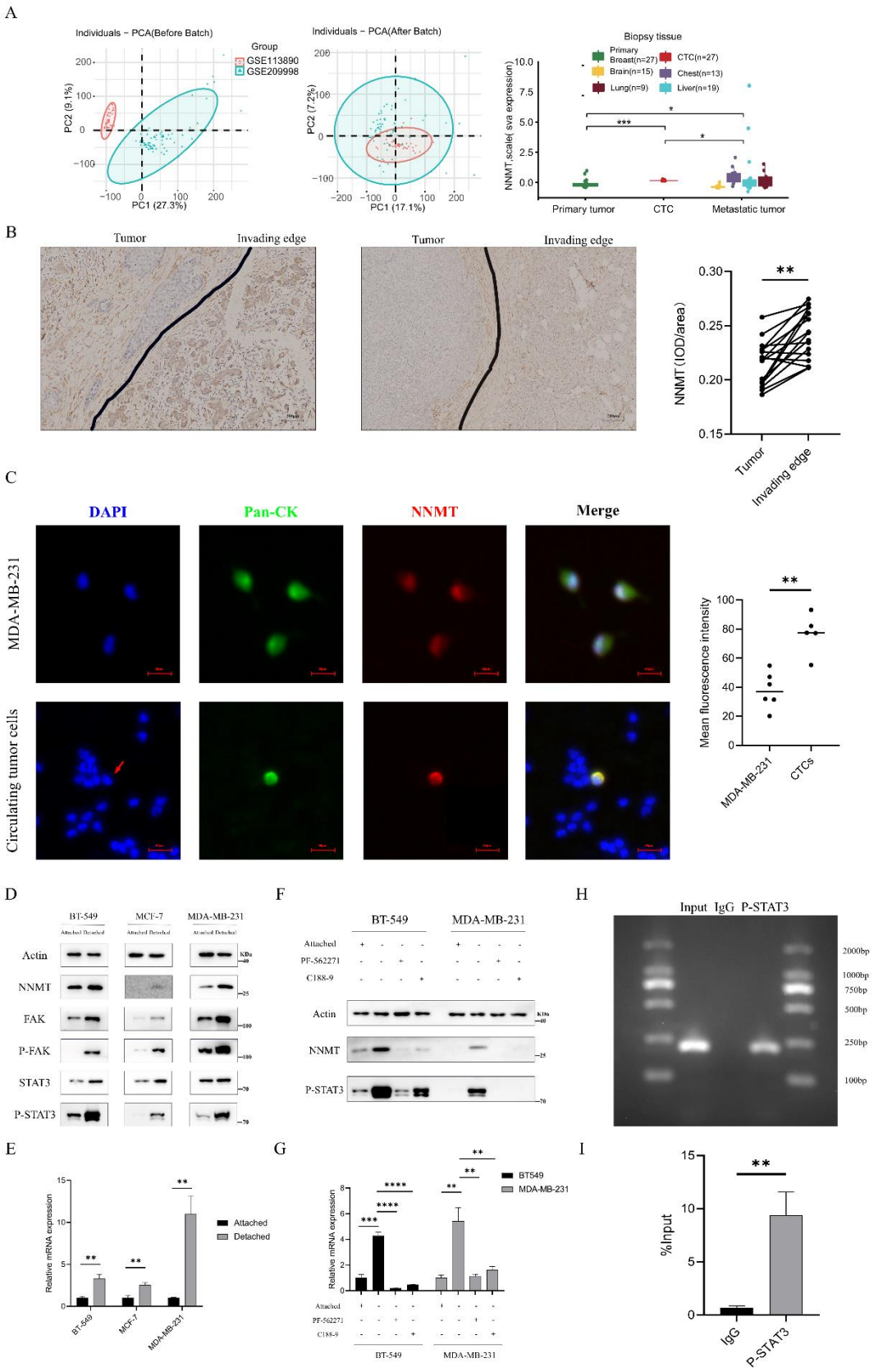

Figure1 **ECM detachment induces NNMT transcription by activating the FAK-STAT3 axis in breast cancer cells.** A: Representative result of sequence data of NNMT expression in primary lesion, CTCs, and metastatic lesions. The scale method

(central standard method: xscaled = (x – x̄) / s) was applied to the data, where x represents the real x-value, x̄ denotes the sample mean, and s represents the sample standard deviation. B: Representative images of NNMT immunohistochemical analysis (100×) and statistical analysis of the integrated optical density of NNMT in the invading edge and tumor of 17 breast cancer patients. Scale bars, 200μm. **P < 0.01. C: Representative and quantitative results of NNMT expression between MDA-MB-231 and isolated CTCs by Immunofluorescence assay. CK^+ and $DAPI^+$ cells indicate circulating tumor cells, while CK^- and $DAPI^+$ cells indicate white blood cells. Scale bars, 50μm. D-E: Representative result of NNMT, STAT3, P-STAT3, FAK, and P-FAK proteins by WB in detached BT-549, MCF-7, and MDA-MB-231 cells. The qPCR results confirmed the upregulation of NNMT in three detached cell lines. F-G: Protein and mRNA levels of NNMT and P-STAT3 after treating detached cells with FAK inhibitor PF-562271 (10μM for 48 hours) and P-STAT3 inhibitor C188-9 (10μM for 48 hours) by WB and qPCR. **P < 0.01, ***P < 0.001, ****P < 0.0001. H-I: ChIP assay showing that P-STAT3 directly binds to NNMT promotor, as detected by PCR and qPCR. **P < 0.01.

3.2 NNMT promotes anoikis resistance in breast cancer cells

To explore the function of NNMT in detached breast cancer cells, we established NNMT-knockdown MDA-MB-231 and BT-549 breast cancer cell lines via lentiviral transfection and NNMT-overexpression MCF-7 and HCC1937 cell models. The effect of NNMT knockdown or overexpression was confirmed at protein and mRNA levels (Supplementary Fig. 2). After culturing these 4 cell lines in suspension for 48 hours, we observed that NNMT overexpression increased cell aggregation while knockdown decreased it (Fig. 2A), indicating the potential role of NNMT in promoting anoikis resistance in detached breast cancer cells. WB analysis of PARP showed that NNMT-knockdown cells showed a higher proportion of anoikis, and NNMT-overexpression cells showed a lower proportion of anoikis (Fig. 2B). Anoikis assay showed that neither NNMT knockdown nor overexpression significantly affect cell apoptosis upon attachment. However, when cancer cells detached from the culture plate, NNMT knockdown significantly decreased cell survival rates in BT-549 (from 8.01% to 27.8%) and MDA-MB-231 (from 3.08 %to 6.4%), while NNMT overexpression protected MCF-7(from 43.3% to 30%) and HCC1937(from 33.1% to 15.34%) from anoikis compared to control group (Fig. 2C). Interestingly, difference in the proportion of anoikis among these 4 cell lines may be associated with their level of natural NNMT expression (Supplementary Fig. 3) since cell lines with high NNMT expression, such as MDA-MB-231 and BT-549, exhibited a low proportion of anoikis while cell lines with low NNMT-expression, such as MCF-7 and HCC1937, exhibited a high proportion of anoikis. Results of soft agar assay showed that NNMT-knockdown in BT-549 and MDA-

299 MB-231 cells significantly increased the number of cell colonies while NNMT-overexpression in
300 MCF-7 and HCC1937 cells decreased the number of cell colonies which were also consistent with our
301 hypothesis (Fig. 2D). To further verify our hypothesis, we constructed a CTC model with MDA-MB-
302 231 cells and results showed that the number of CTCs was significantly reduced in NNMT knockdown
303 group compared with control group (Fig. 2E). These findings demonstrated that NNMT-competent
304 breast cancer cells could resist anoikis and survive during ECM detachment.

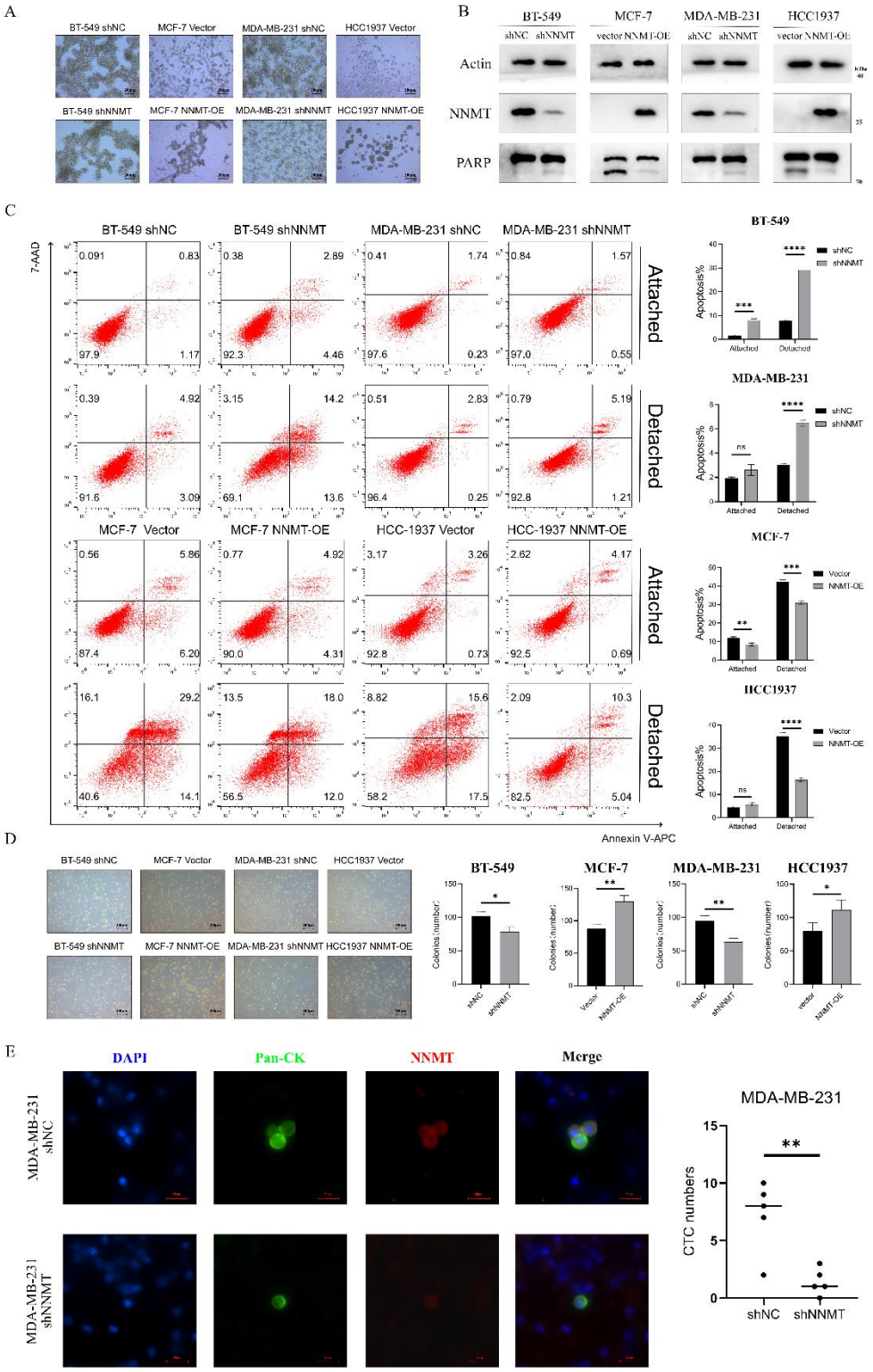

Figure2 **NNMT promotes anoikis resistance in breast cancer cells.** A: Cell morphology after detachment for 48 hours. Scale bar, 100μm. B: Representative results of anoikis levels of BT-549, MCF-7, HCC1937, and MDA-MB-231 cell lines by Annexin V/7-AAD staining after culture on 1% agar plates for 48h. **P < 0.01, ***P < 0.001, ****P < 0.0001. C: WB analysis showed

309 that cleaved-PARP was increased in NNMT-knockdown BT-549 and MDA-MB-231 cells, but decreased in NNMT
310 overexpressing MCF-7 and HCC1937 cells. D: Representative result of soft agar assay of BT-549, MCF-7, MDA-MB-231, and
311 HCC1937. Scale bar, 100μm. *P < 0.05, **P < 0.01. E: Representative and quantitative results of CTCs isolated from MDA-
312 MB-231 shNC and shNNMT injected SCID mouse model by Immunofluorescence assay. CK^+ and $DAPI^+$ cells indicate
313 circulating tumor cells, while CK^- and $DAPI^+$ cells indicate white blood cells. Scale bars, 50μm.

314

315 **3.3 NNMT promoted FAO in attached and detached breast cancer cells.**

316 To investigate the mechanism of breast cancer resistance to anoikis, we preliminarily analyzed
317 differential gene expression in CTCs and non-metastatic breast cancer tissue (Supplementary Table 2).
318 Through enrichment analysis, we found FAO to be among the top 10 dysregulated activation pathways
319 of CTCs (Fig. 3A), indicating its potential role in breast cancer during detachment. Enrichment results
320 of the P-adjust<0.001 pathway are listed in Supplementary Table 3. Moreover, we observed a positive
321 correlation between FAO and NNMT in breast cancer, based on a correlation of 0.525, p<0.05 (Fig. 3B,
322 Supplementary Fig. 4), indicating the possible link between FAO and NNMT in breast cancer. Next, to
323 measure the amount of lipid in the cytoplasm, we performed BODIPY staining and in contrast to
324 respective controls, NNMT-knockdown in BT-549 and MDA-MB-231 cells significantly increased the
325 total amount of lipid, while NNMT overexpression in MCF-7 cells decreased lipid amount (Fig. 3C),
326 suggesting that NNMT may have an effect on lipid catabolism like FAO. To directly investigate FAO
327 activity, we performed an FAO assay with Seahorse XF96e Extracellular Flux Analyzer. After
328 starvation and exogenous palmitate treatment, basal respiration and maximal respiration both decreased
329 in NNMT-knockdown BT-549 cells while maximal respiration increased in NNMT overexpression
330 MCF-7 cells (Fig. 3D). To investigate the effect of NNMT on cellular uptake of fatty acids, the
331 BODIPY lipid uptake assay was performed and the results showed that NNMT-knockdown cells
332 exhibit lower lipid deposit after lipid treatment and NNMT-overexpression cells exhibit higher lipid
333 deposit (Fig. 3E), indicating NNMT may enhance breast cancer lipid uptake. Subsequently, we
334 detected the expression of key metabolic enzymes of the FAO pathway, namely, CPT1A and CD36, in
335 attached and detached cells. Our results showed that protein and mRNA levels of CPT1A and CD36
336 were higher in NNMT-overexpression MCF-7 cells and lower in NNMT-knockdown BT-549 cells
337 under both detachment and attachment, suggesting NNMT can enhancing FAO in detached and
338 attached breast cancer cells (Fig. 3F-G). Similar results were observed in MDA-MB-231 cells, however,

CD36 expression in MDA-MB-231 was too low to be detected by WB (Supplementary Fig. 5). When we used flow cytometry to detect CD36 expression on the cell membrane, results showed that NNMT-knockdown in BT-549 decreased CD36 expression on the cell membrane, while NNMT overexpression in MCF-7 cells decreased CD36 expression (Supplementary Fig. 6). Taken together, these results indicated that NNMT could enhance FAO in breast cancer cells, whether attached or detached.

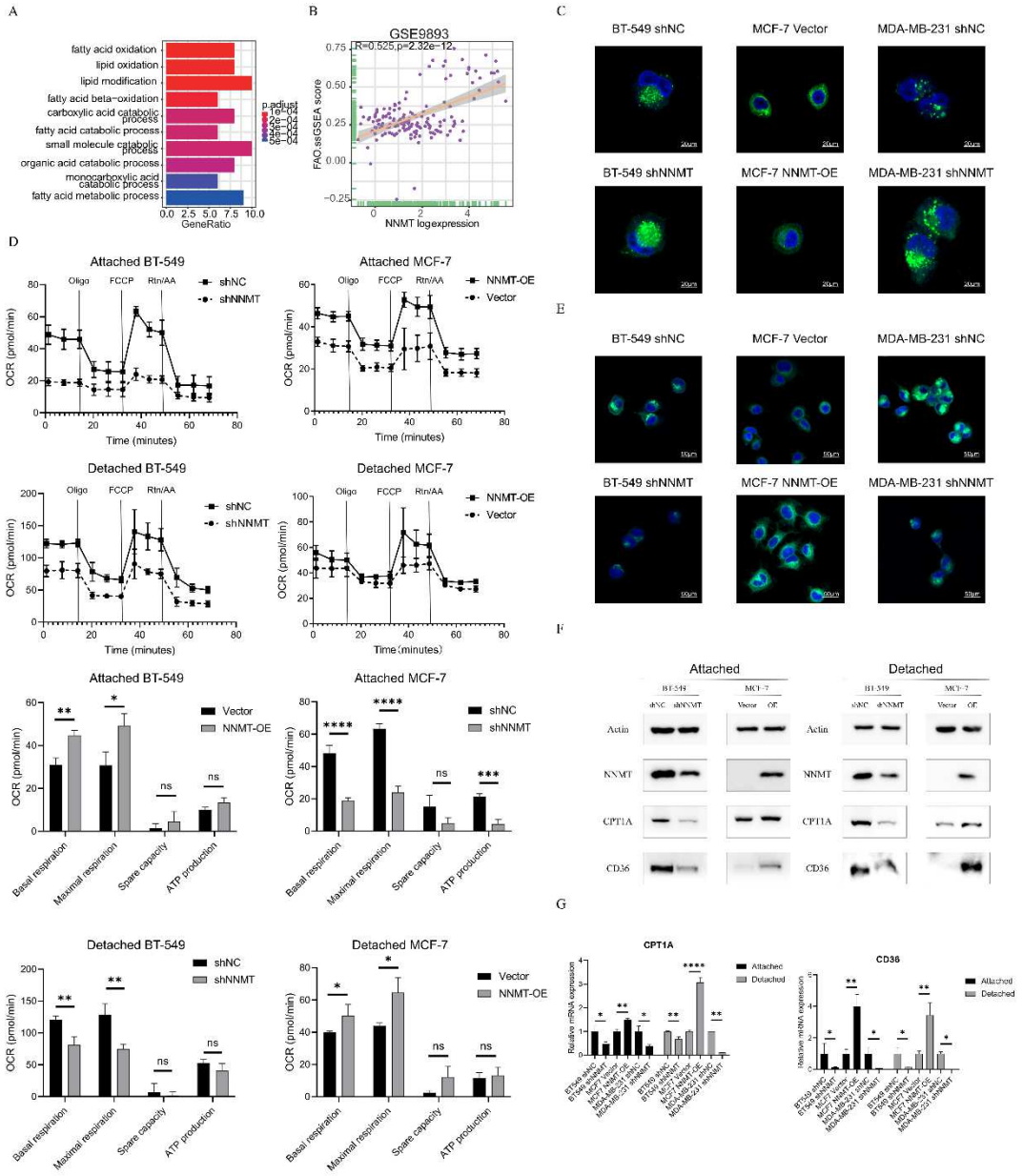

Figure3 **NNMT promoted FAO in attached and detached breast cancer cells.** A: The top 10 NNMT-related pathways among CTCs compared to primary lesions from combined cohorts (GSE4922, GSE9893, and GSE24450). B: Relationship between mRNA expression of the FAO pathway and NNMT in breast cancer patients from combined cohorts. C: Representative results of BODIPY staining in BT-549, MCF-7, and MDA-MB-231 cell models using confocal microscope. D: Measurement of FAO rate

349 in attached and detached BT-549 and MCF-7 cell models using the Seahorse XF96e Extracellular Flux Analyzer. *P < 0.05, **P
350 < 0.01, ****P < 0.0001. E: Representative images of BODIPY lipid uptake in BT-549, MCF-7, and MDA-MB-231 cell models
351 using confocal microscope. F-G: WB and qPCR analysis showed that CPT1A and CD36 were upregulated by NNMT in BT-549
352 and MCF-7, whether detached or not. *P < 0.05, **P < 0.01, ****P < 0.0001

353

354 **3.4 NNMT represses PP2A activity to induce FAO-mediated anoikis resistance**

355 PP2A is considered an important regulator of cancer development since it is a strongly conserved and a
356 major protein phosphatase in mammalian cells[28]. Modulating PP2A will impair tumor metabolic
357 plasticity[29], and methylation of the C-terminal Leu309 residue in its catalytic center will enhance
358 PP2A activity. Since NNMT is a type of methyltransferase which will create metabolic methylation
359 sink[17], we examined the methylation of PP2A expression when NNMT was knocked down or
360 overexpressed. Results showed that the methylation of PP2A was negatively regulated by NNMT with
361 total PP2A unaffected (Fig. 4A). Since PP2A was reported as the negative regulator of both AKT and
362 c-myc[30], while c-myc is reported as a regulator of CPT1A[31] , and since P-AKT is reported as a
363 regulator of CD36[32], we asked if NNMT regulates FAO by the PP2A-AKT/c-myc axis. To
364 investigate this question, we detected the expression of c-myc, and P-AKT in BT-549, MCF-7, MDA-
365 MB-231 cell models and both of them decreased after NNMT knockdown, but increased after NNMT
366 overexpression, indicating the role of NNMT in regulating c-myc and P-AKT (Fig. 4A). Then, we
367 treated NNMT overexpression MCF-7 cells with c-myc inhibitor 10074-G5 and P-AKT inhibitor
368 MK2206. Results showed that the positive regulatory role of NNMT on CPT1A and CD36 expression
369 was mainly achieved by upregulating c-myc and P-AKT (Fig. 4B). In order to investigate whether
370 PP2A methylation plays a critical role in the regulation of AKT and c-myc, we treated BT-549 and
371 MCF-7 cells with the PP2A inhibitor okadaic acid (OA) and PP2A activator perphenazine (PPZ). The
372 results confirmed our hypothesis that NNMT regulates FAO through PP2A-mediated AKT and c-myc
373 activation (Fig. 4C). We next asked if NNMT induced anoikis resistance in breast cancer cells by
374 promoting FAO, we treated NNMT-overexpression MCF-7 cells with FAO inhibitor etomoxir and
375 NNMT-knockdown BT-549 and MDA-MB-231 cells with lipid mixture. As expected, WB assay
376 showed lipid mixture could attenuate anoikis caused by NNMT-knockdown and etomoxir increased
377 anoikis in MCF-7 NNMT-overexpression cells which were consistent with the results of anoikis assay
378 (Fig. 4D). Meanwhile, the soft agar assay showed that etomoxir could significantly decrease the

379 number of cell colonies in NNMT-overexpression cells, whereas lipid mixture increased the number of
380 colonies in NNMT-knockdown cells (Fig. 4E). The results of anoikis assay also showed that etomoxir
381 significantly impaired anoikis resistance in NNMT-overexpression MCF-7 cells (Fig. 4F). Accordingly,
382 lipid mixture could significantly inhibit anoikis of BT-549 and MDA-MB-231 cells deficient in NNMT
383 expression (Fig. 4F).). Taken together, these findings confirmed the hypothesis that NNMT could
384 promote breast cancer cell anoikis resistance by regulating FAO.

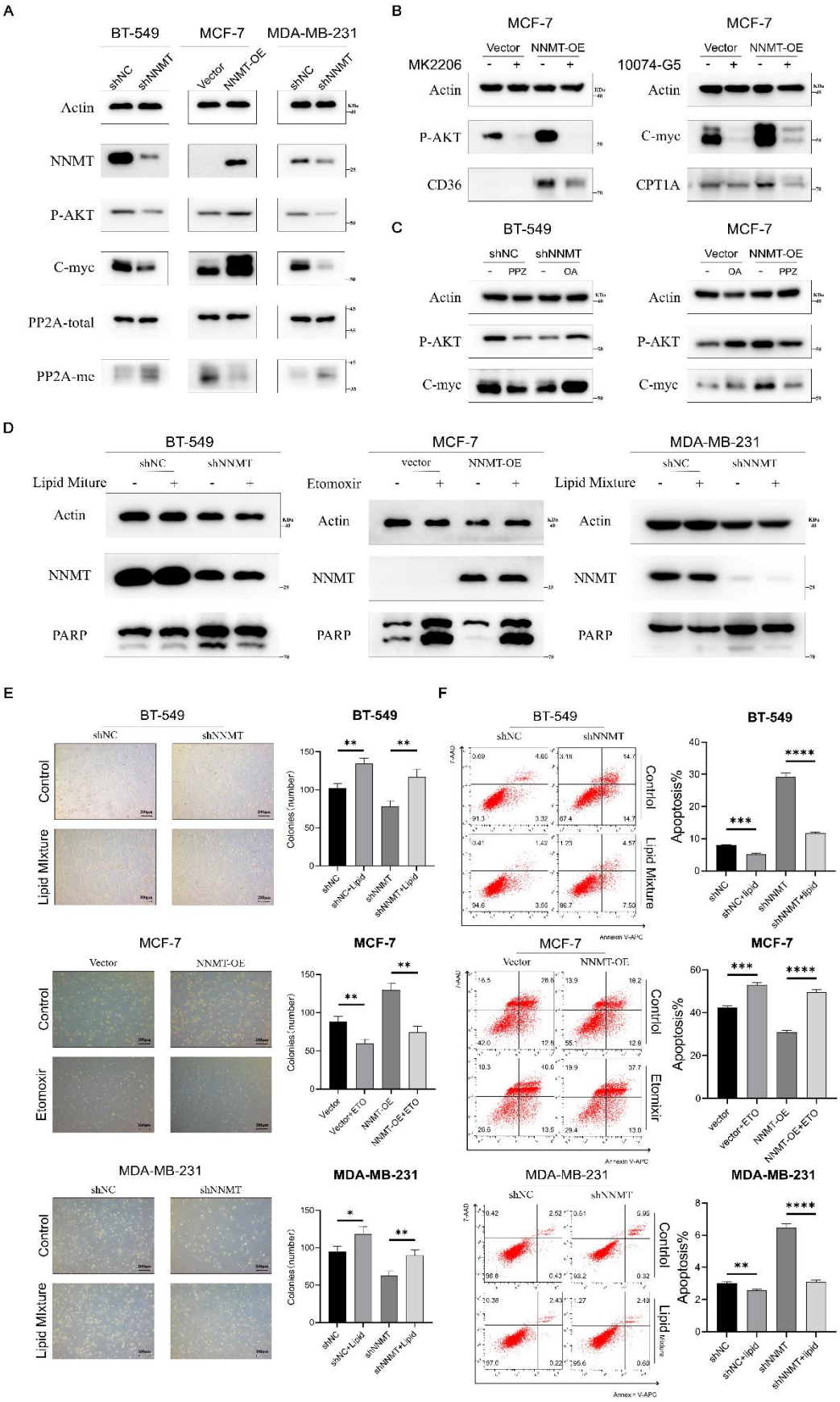
A
BT-549
MCF-7
MDA-MB-231
shNC
shNNMT
Vector
NNMT-OE
Actin
NNMT
P-AKT
C-myc
PP2A-total
PP2A-me
B
MCF-7
Vector
NNMT-OE
MK2206
10074-G5
Actin
P-AKT
CD36
C-myc
CPT1A
C
BT-549
shNC
shNNMT
PPZ
OA
Actin
P-AKT
C-myc
D
BT-549
shNC
shNNMT
Lipid Miture
Actin
NNMT
PARP
MCF-7
vector
NNMT-OE
Etomoxir
MDA-MB-231
Lipid Mixture
E
Control
Lipid Mixture
Etomoxir
Colonies (number)
shNC
shNC+Lipid
shNNMT
shNNMT+Lipid
Vector
Vector+ETO
NNMT-OE
NNMT-OE+ETO
F
Apoptosis%
Annexin V-APC
7-AAD

385

386 Figure4 **NNMT represses PP2A activity to induce FAO-mediated anoikis resistance.** A: Representative WB results of
387 methyl-PP2A, PP2A, p-AKT, C-myc, and NNMT expression in BT-549, MCF-7, and MDA-MB-231 cell models. B:
388 Representative result of P-AKT, c-myc, CD36 and CPT1A proteins by Western blotting in the MCF-7 cell model with MK2206
389 (1μM for 48 hours) and 10074-G5 (10μM for 48 hours) treatment. C: Representative result of P-AKT and c-myc proteins by
390 Western blotting in the MCF-7 and BT-549 cell models with PPZ (25μM for 48 hours) or OA (0.25μM for 48 hours) treatment.
391 D-F: Representative result of anoikis levels in BT-549, MCF-7, and MDA-MB-231 cell lines with etomoxir (100μM for 48 hours)
392 or lipid mixture treatment (2% for 48 hours) by flow cytometry, Western blot, and soft agar assay. *P < 0.05, **P < 0.01, ***P <
393 0.001, ****P < 0.0001.

394

395 **3.5 NNMT-mediated FAO induced anoikis resistance by ROS clearance**

396 Compared with attached cancer cells, detached cells exhibit a higher level of ROS, which triggers
397 anoikis and hinders cancer metastasis [33]. Therefore, metastatic cancer cells always reduce oxidative
398 stress to remain viable during detachment[34].FAO is a crucial source of cellular NADPH, which
399 maintains redox homeostasis (Fig. 5A). Thus, we next measured ROS levels in detached breast cancer
400 cells. As expected, ROS accumulation was much higher in detached BT-549 NNMT-knockdown cells
401 than control group, whereas detached NNMT-overexpression MCF-7 cells showed less ROS
402 accumulation (Fig. 5B). Also, ROS accumulation decreased in BT-549 NNMT-knockdown cells
403 treated with lipid mixture, while etomoxir treatment significantly restrained the effect of NNMT on
404 ROS clearance in NNMT-overexpression MCF-7 cells (Fig. 5C). Furthermore, the $NADPH/NADP^+$
405 ratio in BT-549 NNMT-knockdown cells did not persist after detachment (Fig. 5D), which was
406 consistent with the higher ROS accumulation observed in detached NNMT-knockdown BT-549 cells.
407 In contrast, NNMT-overexpressing MCF-7 cells were more capable of maintaining redox homeostasis
408 by stabilizing $NADPH/NADP^+$ ratio, and this effect was suppressed by etomoxir (Fig. 5D). Moreover,
409 NAC (N-acetyl-L-cysteine) treatment, one of the ROS scavengers, rescued the number of colonies of
410 BT-549 shNNMT cells in the soft agar assay (Fig. 5E). These results demonstrated that ROS
411 elimination via NNMT-mediated FAO was critical to anoikis resistance in breast cancer cells and,
412 further, that targeting this pathway may hold therapeutic potential.

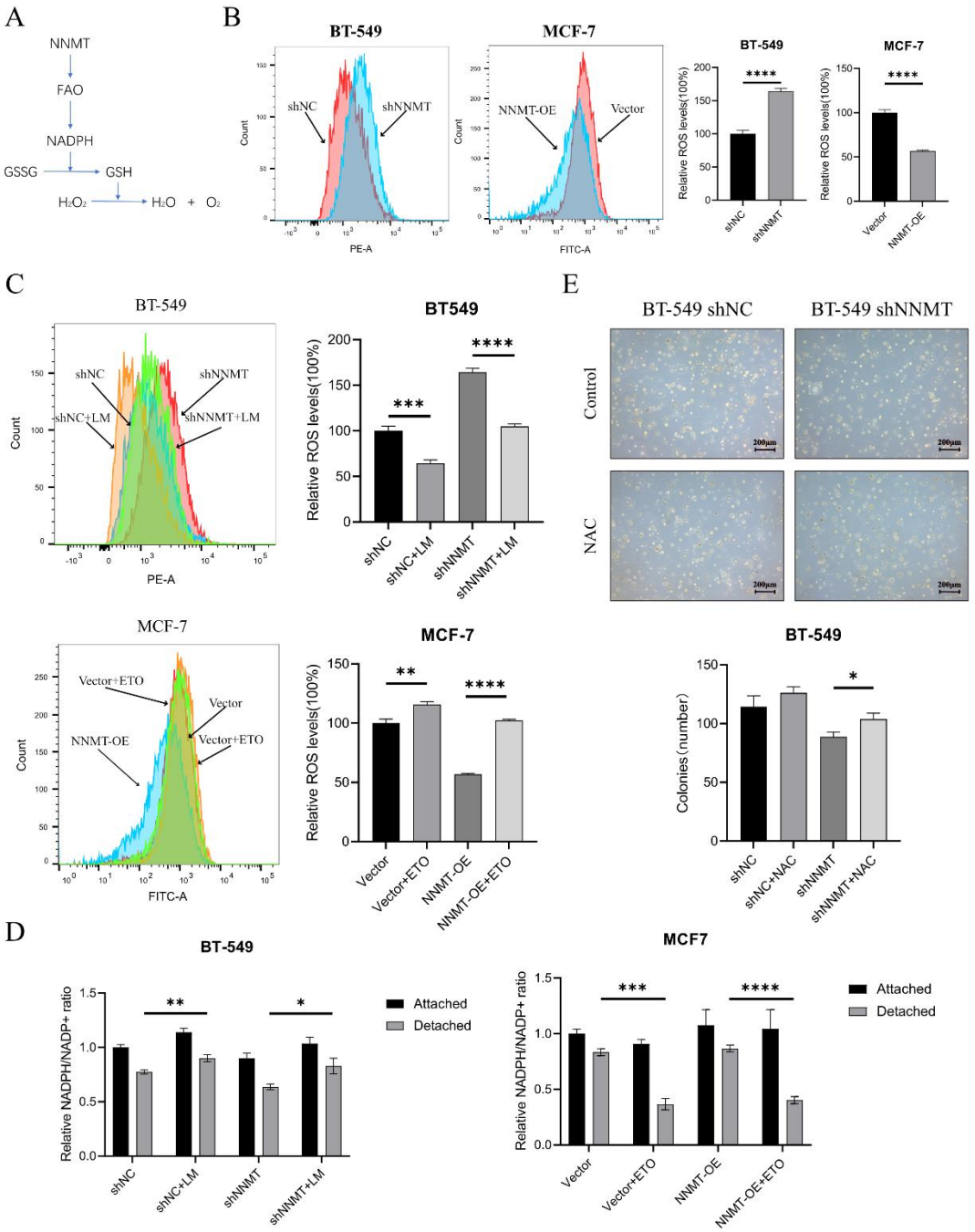

Figure5 **NNMT-mediated FAO induction of anoikis resistance by ROS clearance**. A: Graphical description of the relationship among NNMT, FAO, and ROS elimination. B: Representative results of basic ROS levels in detached BT-549 and MCF-7 cell lines by DCF-DA or DHE staining. ****P < 0.0001. C: Representative result of ROS levels in detached BT-549 and MCF-7 cell lines after etomoxir or lipid mixture treatment by DCF-DA or DHE staining. **P < 0.01, ***P < 0.001, ****P < 0.0001. D: NADPH/NADP+ ratio was determined in attached and detached MCF-7 and BT-549 cell models. *P < 0.05, **P < 0.01, ***P < 0.001, ****P < 0.0001. E: Representative images of NAC, a ROS scavenger, treatment on the BT-549 cell model in soft agar

421

422 **3.6 Inhibition of FAO by targeting NNMT decreased metastatic formation in vivo**

423 To investigate whether NNMT affected breast cancer cell metastasis *in vivo*, the lung metastasis
424 model was constructed with MDA-MB-231 or E0771 cell lines, and mice were administered 40 mg/kg
425 etomoxir or vehicle intraperitoneally every two days. The results of MDA-MB-231 lung metastasis
426 showed that mice injected with NNMT-knockdown cells exhibited fewer pulmonary metastatic
427 nodules than the control group (Fig. 6A-B). These results also illustrated that etomoxir significantly
428 inhibited pulmonary metastatic nodule formation (Fig. 6A-B), while the body weight of the mice was
429 not obviously affected (Supplementary Fig. 7A). In the E0771 lung metastasis model, NNMT
430 overexpression increased the number of metastatic nodules, and treatment with etomoxir significantly
431 suppressed the increase of metastatic lesions caused by NNMT (Fig. 6C-D). To visualize the effects of
432 NNMT on MCF-7 cell anoikis resistance *in vivo*, we labeled MCF-7 vector or NNMT overexpression
433 cells with CellTracker Green the and injected them into SCID mice via the tail vein. Lung tissues were
434 collected at 4 hours and 24 hours after injection and then processed into frozen sections, which were
435 stained with DAPI for fluorescence microscopy. The results revealed a significant increase in the
436 number of cancer cells in the lungs at 24 hours after NNMT overexpression, while etomoxir treatment
437 suppressed the increase of survival cell number (Fig. 6E-F). These findings demonstrated that NNMT-
438 mediated FAO played an essential role in the anoikis resistance of breast cancer. To assess the effect of
439 NNMT on FAO, we measured CPT1A and NNMT expression in the lung metastases of mice (Fig. 6G-
440 H). CD36 was too faint to be detected in MDA-MB-231 cells, which is consistent with the results in
441 the cell model. Additionally, the effect of JBNSF-000088, one of NNMT inhibitors, was also tested in
442 the lung metastasis model and results showed its inhibitory effect on metastatic nodule formation
443 (Supplementary Fig. 8). Furthermore, the previously reported NNMT inhibitors Curcumin[35] and
444 Vanillin[16] also showed promising therapeutic potential in the inhibition of metastasis
445 formation(Supplementary Fig. 8). Overall, NNMT played an essential role in the fatty acid metabolism
446 of detached breast cancer cells to maintain redox homeostasis (Fig. 6I). Therefore, targeting NNMT
447 could effectively stimulate anoikis and suppress breast cancer metastasis.

448

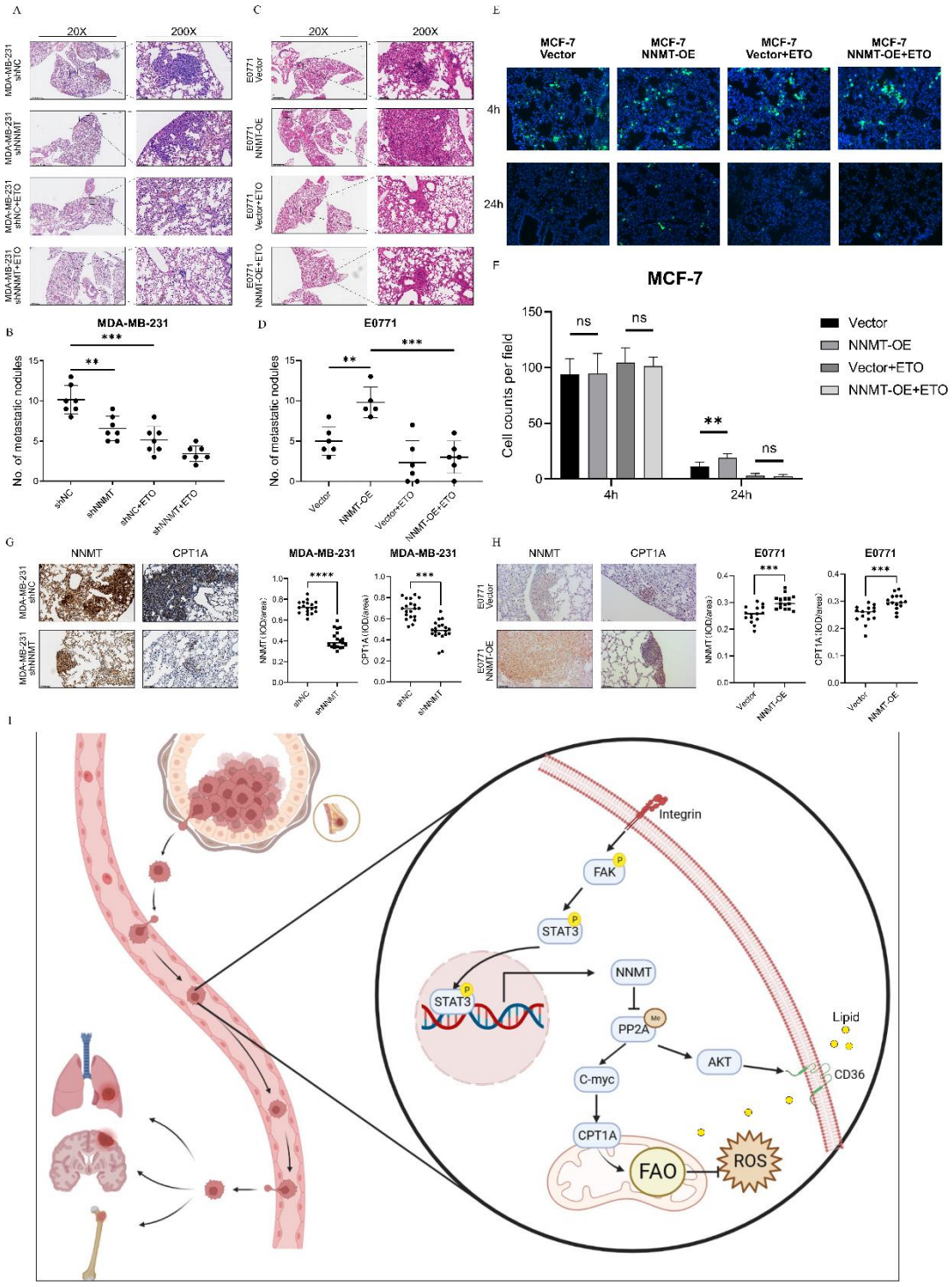

Figure6 The inhibition of FAO by targeting NNMT decreased metastatic formation in vivo. A-B: The image of H&E staining of lungs harvested after injecting shNC and shNNMT MDA-MB-231 cells through the tail vein. Results showed that inhibition of FAO by NNMT-knockdown or etomoxir significantly reduced the size and number of lung metastatic nodules in mouse model. Scale bar (20×), 1250μm. Scale bar (200×), 100μm. C-D: The image of H&E staining for Lungs harvested after injecting E0771 vector and NNMT-OE cells through the tail vein and results showed that NNMT overexpression increased the number of metastatic nodules, and etomoxir treatment suppressed the increase of metastatic nodules caused by NNMT. Scale bar

(20×), 1250μm. Scale bar (200×), 100μm. E-F: The fluorescent image of the lung frozen sections 4h or 24h after injecting CellTracker Green labeled MCF-7 cells and results revealed a significant increase in the number of cancer cells in the lungs at 24 hours after NNMT overexpression, while etomoxir treatment suppressed the number of surviving cancer cells. G-H: Representative result of CPT1A and NNMT expressions in lungs harvested from two groups by IHC. Scale bar (200×), 100μm. I: A graphic representation showing that detachment-induced NNMT protects breast cancer cells against anoikis by enhancing FAO.

4. Discussion

Anoikis is a specific form of programmed cell death triggered by cell detachment from ECM, working as a critical protective mechanism in preventing adherent-independent cell survival and attachment to an inappropriate ECM[36]. Thus, the ability to resist anoikis has become a significant focus of research attention. To survive in the inappropriate ECM, cancer cells initiate a constitutive activation of pro-survival signaling and alter their metabolic pathway to meet energy demands[6]. Sustained activation of the integrin signaling pathway is one of the most common mechanisms to achieve anoikis resistance in cancer cells. Integrins contribute to signal transduction from extracellular to intracellular such as the phosphorylation of downstream molecules like FAK, PI3K, and MAPK[37]. Our study revealed that NNMT was upregulated by the integrin/FAK-STAT3 axis in detached breast cancer cells, suggesting that NNMT may participate in the integrin/FAK-mediated anoikis resistance. Consistently, our *in vitro* experiments showed that NNMT knockdown led to decreased survival of detached breast cancer cells, while NNMT overexpression resulted in enhanced survival and anoikis resistance of the detached breast cancer cells. Interestingly, our findings demonstrated that BT-549 and MDA-MB-231 cells, which express high levels of NNMT, exhibit significantly lower levels of anoikis compared to MCF-7 and HCC1937 cells, which express lower levels of NNMT. This finding further supports our hypothesis.

Metabolic reprogramming is required to meet the energy demands of cancer cells to support tumor metastasis. The metabolic switch from anabolism (glycolysis and fatty acid synthesis) to catabolism (FAO) is required to help cells evade anoikis[8,38]. For instance, metastatic HCC cells reprogrammed the anabolic/catabolic balance from aerobic glycolysis towards AMPK-activated FAO to resist anoikis[39]. CPT1A, the FAO rate-limiting enzyme, has been shown to facilitate esophageal squamous cell carcinoma cells in resisting anoikis by maintaining redox homeostasis[40]. Accordingly, our study

485 demonstrates that NNMT may mediate the metabolic reprogramming toward FAO in breast cancer.
486 However, the role of NNMT in fatty acid metabolism is still controversial. Studies have shown that
487 NNMT can regulate hepatic nutrient metabolism by stabilizing Sirt1 and that liver NNMT expression
488 inversely correlates with total cholesterol, LDL cholesterol, and TG levels in serum, as well as other
489 parameters in both human and mice [41]. Furthermore, nicotinamide, the NNMT substrate, may cause
490 loss of body weight in rats by reducing food intake and food efficiency decrease at pharmacological
491 doses [42]. Conversely, 1-MNA, the NNMT product, can improve the metabolic profile of mice fed
492 with a high-fat diet[43]. Other researchers hold conflicting views. For instance, Kraus reported that
493 NNMT knockdown in white adipose tissue and liver protected against diet-induced obesity by
494 increasing cellular energy expenditure[18], and Xu demonstrated that NNMT promoted lipid
495 accumulation in 3T3-L1 adipocytes[44]. Therefore, further experiments are needed to clarify the
496 specific function of NNMT. In this study, we found that NNMT could upregulate CPT1A, the FAO
497 rate-limiting enzyme, and CD36, one of the lipid uptake receptors. Therefore, NNMT may contribute
498 to both lipid catabolism and lipid accumulation, which may explain the controversial effects of NNMT
499 in lipid metabolism. Despite the lack of consensus, tumors are well known as heterogeneous entities
500 consisting of cancer cells with varying metabolic states. It is also well recognized that cancer cells can
501 optimize the exploitation of limited energy resources(40), particularly when cells undergo ECM
502 detachment.

503 Since its discovered in 1984, NNMT has been reported to participate in cancer development and
504 progression[46,47]. In our previous research, we demonstrated that NNMT can promote cancer cell
505 migrations[24], but the complete role of NNMT in metastasis is still not fully understood. Cancer
506 metastasis is a complex multi-step process including local invasion, intravasation, survival in the
507 circulation, extravasation, and metastatic colonization[48]. This study aimed to investigate the function
508 of NNMT in breast cancer anoikis resistance, and we revealed that NNMT can maintain redox
509 homeostasis by enhancing FAO to attenuate breast cancer anoikis. Moreover, our previous studies have
510 shown that the catalytic product of NNMT, 1-MNA, could attenuate ROS production by the ASK1-p38
511 MAPK pathway [49], and in this study, our data shows that the ROS scavenging effect of NNMT may
512 be partially achieved through enhancing FAO, whereas 1-MNA has no obvious effect on CPT1A or
513 CD36 (Supplementary Fig. 9). These findings may provide a novel perspective in the understanding of
514 the role NNMT plays in cancer metastasis.

Cancer cells rely on the reprogramming of cellular metabolism to facilitate malignant growth[50]. Therefore, cancer metabolism is an emerging crucial issue in clinical research. Recently, FAO has received increasing attention in the field of tumor metabolic therapy, and etomoxir was reported to significantly suppress multiple cancer development in a FAO-dependent way(47-48). Our data also indicated that etomoxir could reverse anoikis resistance induced by NNMT in the lung metastasis model. Although etomoxir has been reported to induce myocardial hypertrophy and hepatocellular injury[53], obvious weight reduction is not observed. Moreover, we also investigated the impact of the NNMT antagonists JBNSF088, Curcumin, and Vanillin on the breast cancer metastasis model. Overall, our results demonstrate that inhibiting NNMT represents a promising strategy for treating breast cancer.

5. Conclusion

In conclusion, this study offers novel insight into the molecular mechanisms underlying anoikis resistance in breast cancer. We found that the upregulation of NNMT in detached breast cancer is caused by activation of the FAK-STAT3 axis and that NNMT enhances FAO to maintain redox balance during detachment. Therefore, our findings suggest that NNMT may be a viable therapeutic target for metastatic breast cancer. Further research is required to elucidate the specific pathways involved in breast cancer metastasis, thereby improving overall patient survival.

Author contributions

TQC was responsible for validation, formal analysis, writing original draft and review & editing. MYL was responsible for investigation, writing original draft and review & editing. GYZ was responsible for investigation, data analysis. ZL and FQ was responsible for investigation. FSN was responsible for investigation, data curation. ZR was responsible for investigation, data curation. ZJ (Zeng Jin) was responsible for investigation, data curation. LGL was responsible for methodology. XXY was responsible for investigation, conceptualization. WYZ was responsible for review & editing. ZJ (Zhang Jun) was responsible for conceptualization, supervision, funding acquisition.

Funding

This work was supported by grants from the National Natural Science Foundation of China (82172362, 81271914, and 81800023), China Scholarship Council (201906325012), Key Research and Development Program of Zhejiang Province (2019C03021 and 2022C03037), Natural Science Foundation of Zhejiang Province (LY24H200001 and LY22H200002), Health Bureau Foundation of Zhejiang Province (2024KY1104) and Key Laboratory of Precision Medicine in Diagnosis and Monitoring Research of Zhejiang Province (2022E10018)

Acknowledgements

We thank Dr. Kaishan Zhang and Dr. Chao Li, the Research and Development Center of Wastonbiotech, for their assistance with CTC isolation. We also thank Prof. Xiangwei Gao, Zhejiang University School of Medicine, for discussion and editorial assistance.

Data Availability

The data generated and/or analyzed during this study are available from the corresponding author on reasonable request

Declarations

Ethical approval and consent to participate

The animal experiment was approved by the Institutional Animal Care and Use Committee of Sir Run Run Shaw Hospital and was performed in accordance with the National Advisory Committee for Laboratory Animal Research (NACLAR) Guidelines (IACUC Number: 2928). Patient studies were performed in accordance with the ethical guidelines of the Declaration of Helsinki.

566 **Consent for publication**

567 All authors have read the manuscript and agree to publish.

568

569 **Competing Interests**

570 The authors declare no competing interests

571

572

573 **Reference**

574 1. H. Sung, J. Ferlay, R. L. Siegel, M. Laversanne, I. Soerjomataram, A. Jemal, and F. Bray, CA.
575 Cancer J. Clin. **71**, 209 (2021).
576 2. Y. Liang, H. Zhang, X. Song, and Q. Yang, Semin. Cancer Biol. **60**, 14 (2020).
577 3. The Cancer Genome Atlas Network, Nature **490**, 61 (2012).
578 4. S. M. Frisch and R. A. Screaton, Curr. Opin. Cell Biol. **13**, 555 (2001).
579 5. A. Tajbakhsh, M. Rivandi, S. Abedini, A. Pasdar, and A. Sahebkar, Crit. Rev. Oncol. Hematol. **140**,
580 17 (2019).
581 6. J. A. Mason, K. R. Hagel, M. A. Hawk, and Z. T. Schafer, Trends Cancer **3**, 475 (2017).
582 7. Q. Qu, F. Zeng, X. Liu, Q. J. Wang, and F. Deng, Cell Death Dis. **7**, e2226 (2016).
583 8. Y. Wang, Z. Zeng, J. Lu, Y. Wang, Z. Liu, M. He, Q. Zhao, Z. Wang, T. Li, Y. Lu, Q. Wu, K. Yu, F.
584 Wang, H.-Y. Pu, B. Li, W. Jia, M. shi, D. Xie, T. Kang, P. Huang, H. Ju, and R. Xu, Oncogene **37**,
585 6025 (2018).
586 9. T. Wang, J. F. Fahrmann, H. Lee, Y.-J. Li, S. C. Tripathi, C. Yue, C. Zhang, V. Lifshitz, J. Song, Y.
587 Yuan, G. Somlo, R. Jandial, D. Ann, S. Hanash, R. Jove, and H. Yu, Cell Metab. **27**, 136 (2018).
588 10. M. P. De Oliveira and M. Liesa, Cells **9**, 2600 (2020).
589 11. W. Zhou, M. Gui, M. Zhu, Z. Long, L. Huang, J. Zhou, L. He, and K. Zhong, Oncol. Lett. **8**, 1175
590 (2014).
591 12. X. Xie, H. Yu, Y. Wang, Y. Zhou, G. Li, Z. Ruan, F. Li, X. Wang, H. Liu, and J. Zhang, Arch.
592 Biochem. Biophys. **564**, 52 (2014).
593 13. Y. Wang, J. Zeng, W. Wu, S. Xie, H. Yu, G. Li, T. Zhu, F. Li, J. Lu, G. Y. Wang, X. Xie, and J.
594 Zhang, Breast Cancer Res. **21**, 64 (2019).
595 14. J. Yang, Q. Tong, Y. Zhang, S. Yuan, Y. Gao, K. Deng, Y. Wang, J. Lu, X. Xie, Z. Zhang, and J.
596 Zhang, J. Cancer **12**, 6170 (2021).
597 15. Y. Hah, H. Cho, S. Jo, Y. Park, E. Heo, and T. Yoon, Oncol. Rep. (2019).
598 16. G. Li, B. Kong, Q. Tong, Y. Li, L. Chen, J. Zeng, H. Yu, X. Xie, and J. Zhang, Oncol. Rep. **45**, 110
599 (2021).
600 17. O. A. Ulanovskaya, A. M. Zuhl, and B. F. Cravatt, Nat. Chem. Biol. **9**, 300 (2013).
601 18. D. Kraus, Q. Yang, D. Kong, A. S. Banks, L. Zhang, J. T. Rodgers, E. Pirinen, T. C. Pulinilkunnil,
602 F. Gong, Y. Wang, Y. Cen, A. A. Sauve, J. M. Asara, O. D. Peroni, B. P. Monia, S. Bhanot, L.
603 Alhonen, P. Puigserver, and B. B. Kahn, Nature **508**, 258 (2014).
604 19. M. A. Eckert, F. Coscia, A. Chryplewicz, J. W. Chang, K. M. Hernandez, S. Pan, S. M. Tienda, D.
605 A. Nahotko, G. Li, I. Blaženović, R. R. Lastra, M. Curtis, S. D. Yamada, R. Perets, S. M. McGregor, J.
606 Andrade, O. Fiehn, R. E. Moellering, M. Mann, and E. Lengyel, Nature **569**, 723 (2019).
607 20. Y. Cui, D. Yang, W. Wang, L. Zhang, H. Liu, S. Ma, W. Guo, M. Yao, K. Zhang, W. Li, Y. Zhang,
608 and F. Guan, Mol. Carcinog. **59**, 940 (2020).
609 21. A. Zhu, Y. Shan, J. Zhang, X. Liu, R. Ying, and W. Kong, Kaohsiung J. Med. Sci. **37**, 305 (2021).

22. A. Reustle, L. Menig, P. Leuthold, U. Hofmann, V. Stühler, C. Schmees, M. Becker, M. Haag, V. Klumpp, S. Winter, F. A. Büttner, S. Rausch, J. Hennenlotter, F. Fend, M. Scharpf, A. Stenzl, J. Bedke, M. Schwab, and E. Schaeffeler, Clin. Transl. Med. **12**, (2022).
23. J. Zhang, Y. Wang, G. Li, H. Yu, and X. Xie, PLoS ONE **9**, e89202 (2014).
24. Y. Wang, X. Zhou, Y. Lei, Y. Chu, X. Yu, Q. Tong, T. Zhu, H. Yu, S. Fang, G. Li, L. Wang, G. Y. Wang, X. Xie, and J. Zhang, Cancer Lett. **547**, 215884 (2022).
25. L. Jin, J. Chun, C. Pan, A. Kumar, G. Zhang, Y. Ha, D. Li, G. N. Alesi, Y. Kang, L. Zhou, W.-M. Yu, K. R. Magliocca, F. R. Khuri, C.-K. Qu, C. Metallo, T. K. Owonikoko, and S. Kang, Mol. Cell **69**, 87 (2018).
26. M. Tomida, H. Ohtake, T. Yokota, Y. Kobayashi, and M. Kurosumi, J. Cancer Res. Clin. Oncol. **134**, 551 (2008).
27. D. Cao, Z. Qi, Y. Pang, H. Li, H. Xie, J. Wu, Y. Huang, Y. Zhu, Y. Shen, Y. Zhu, B. Dai, X. Hu, D. Ye, and Z. Wang, Cancer Res. **79**, 2604 (2019).
28. N. Wlodarchak and Y. Xing, Crit. Rev. Biochem. Mol. Biol. **51**, 162 (2016).
29. M. Elgendy, M. Cirò, A. Hosseini, J. Weiszmann, L. Mazzarella, E. Ferrari, R. Cazzoli, G. Curigliano, A. DeCensi, B. Bonanni, A. Budillon, P. G. Pelicci, V. Janssens, M. Ogris, M. Baccarini, L. Lanfrancone, W. Weckwerth, M. Foiani, and S. Minucci, Cancer Cell **35**, 798 (2019).
30. E. Kashani and E. Vassella, Cancers **14**, 5227 (2022).
31. J. C. Casciano, C. Perry, A. J. Cohen-Nowak, K. D. Miller, J. Vande Voorde, Q. Zhang, S. Chalmers, M. E. Sandison, Q. Liu, A. Hedley, T. McBryan, H.-Y. Tang, N. Gorman, T. Beer, D. W. Speicher, P. D. Adams, X. Liu, R. Schlegel, J. G. McCarron, M. J. O. Wakelam, E. Gottlieb, A. V. Kossenkov, and Z. T. Schug, Br. J. Cancer **122**, 868 (2020).
32. C.-S. Lin, F.-Y. Lin, L.-J. Ho, C.-S. Tsai, S.-M. Cheng, W.-L. Wu, C.-Y. Huang, C.-H. Lian, S.-P. Yang, and J.-H. Lai, Cardiovasc. Res. **95**, 346 (2012).
33. Z. T. Schafer, A. R. Grassian, L. Song, Z. Jiang, Z. Gerhart-Hines, H. Y. Irie, S. Gao, P. Puigserver, and J. S. Brugge, Nature **461**, 109 (2009).
34. X. Zhou, L. Li, X. Guo, C. Zhang, Y. Du, T. Li, K. Tong, C. Zhu, and Z. Wang, Npj Breast Cancer **8**, 7 (2022).
35. G. Li, S. Fang, X. Shao, Y. Li, Q. Tong, B. Kong, L. Chen, Y. Wang, J. Yang, H. Yu, X. Xie, and J. Zhang, Biomolecules **11**, 1295 (2021).
36. P. Paoli, E. Giannoni, and P. Chiarugi, Biochim. Biophys. Acta BBA - Mol. Cell Res. **1833**, 3481 (2013).
37. S. Sakamoto and N. Kyprianou, Mol. Aspects Med. **31**, 205 (2010).
38. Y. Tan, K. Lin, Y. Zhao, Q. Wu, D. Chen, J. Wang, Y. Liang, J. Li, J. Hu, H. Wang, Y. Liu, S. Zhang, W. He, Q. Huang, X. Hu, Z. Yao, B. Liang, W. Liao, and M. Shi, Theranostics **8**, 5452 (2018).
39. H. Zhao, G. Yan, L. Zheng, Y. Zhou, H. Sheng, L. Wu, Q. Zhang, J. Lei, J. Zhang, R. Xin, L. Jiang, X. Zhang, Y. Chen, J. Wang, Y. Xu, D. Li, and Y. Li, Theranostics **10**, 6483 (2020).
40. T. Tian, Y. Lu, J. Lin, M. Chen, H. Qiu, W. Zhu, H. Sun, J. Huang, H. Yang, and W. Deng, Redox Biol. **58**, 102544 (2022).
41. S. Hong, J. M. Moreno-Navarrete, X. Wei, Y. Kikukawa, I. Tzameli, D. Prasad, Y. Lee, J. M. Asara, J. M. Fernandez-Real, E. Maratos-Flier, and P. Pissios, Nat. Med. **21**, 887 (2015).
42. Y. A. Kang-Lee, R. W. McKEE, S. M. Wright, M. E. Swendseid, D. J. Jenden, and R. S. Jope, (2018).
43. Z. Song, X. Zhong, M. Li, P. Gao, Z. Ning, Z. Sun, and X. Song, Front. Cardiovasc. Med. **8**, 721814 (2021).
44. W. Xu, L. Hou, P. Li, and L. Li, Bioengineered **13**, 12421 (2022).
45. C. E. Griguer, C. R. Oliva, and G. Y. Gillespie, J. Neurooncol. **74**, 123 (2005).
46. R. Seifert, J. Hoshino, and H. Kroger, Biochim. Biophys. Acta BBA - Gen. Subj. **801**, 259 (1984).
47. J. H. Shin, C. W. Park, G. Yoon, S. M. Hong, and K. Y. Choi, Oncogenesis **7**, 58 (2018).
48. S. Valastyan and R. A. Weinberg, Cell **147**, 275 (2011).
49. X. Xie, H. Liu, Y. Wang, Y. Zhou, H. Yu, G. Li, Z. Ruan, F. Li, X. Wang, and J. Zhang, (n.d.).
50. N. M. Anderson, P. Mucka, J. G. Kern, and H. Feng, Protein Cell **9**, 216 (2018).
51. S. Cheng, G. Wang, Y. Wang, L. Cai, K. Qian, L. Ju, X. Liu, Y. Xiao, and X. Wang, Clin. Sci. **133**, 1745 (2019).
52. Z. Tan, L. Xiao, M. Tang, F. Bai, J. Li, L. Li, F. Shi, N. Li, Y. Li, Q. Du, J. Lu, X. Weng, W. Yi, H. Zhang, J. Fan, J. Zhou, Q. Gao, J. N. Onuchic, A. M. Bode, X. Luo, and Y. Cao, Theranostics **8**, 2329 (2018).
53. C. J. F. Holubarsch, M. Rohrbach, M. Karrasch, E. Boehm, L. Polonski, P. Ponikowski, and S. Rhein, Clin. Sci. **113**, 205 (2007).

Supplementary Files

This is a list of supplementary files associated with this preprint. Click to download.

- SupTables.xlsx
- supplementaryfigures.docx